Orientation-sensitive nonlinear growth of graphene: An epitaxial growth mechanism determined by geometry

Huijun Jiang, Ping Wu, Zhonghuai Hou,* Zhenyu Li,† and Jinlong Yang
Department of Chemical Physics & Hefei National Laboratory for Physical Sciences at Microscales, University of Science and Technology of China, Hefei, Anhui 230026, China
(Received 5 February 2013; published 29 August 2013)

Although the corresponding carbon-metal interactions can be very different, a similar nonlinear growth behavior of graphene has been observed for different metal substrates. To understand this interesting experimental observation, a multiscale "standing-on-the-front" kinetic Monte Carlo study is performed. An extraordinary robust geometry effect is identified, which solely determines the growth kinetics and makes the details of carbon-metal interaction not relevant at all. Based on such a geometry-determined mechanism, the epitaxial growth behavior of graphene can be easily predicted in many cases. As an example, the orientation-sensitive growth kinetics of graphene on an Ir(111) surface has been studied. Our results demonstrate that the lattice mismatch pattern at the atomic level plays an important role in macroscopic epitaxial growth.

DOI: 10.1103/PhysRevB.88.054304 PACS number(s): 73.22.Pr, 81.05.ue, 81.15.Aa

I. INTRODUCTION

Due to its excellent electronic, mechanical, thermal, and optical performance, graphene has drawn considerable attention among physicists, chemists, and material scientists.[1] Of the several ways to produce graphene,[1,2] epitaxial growth on metal surfaces is of particular importance because it can generate a large size graphene sample of high quality.[3–7] Plenty of nontrivial growth behaviors have been revealed in experiments.[3,8–14] Of particular interest, the growth rate is found to be a quintic function of carbon monomer concentration on the main growth orientation (R0 orientation) of an Ir(111) surface, which suggests a growth mechanism with the attachment of five-atom clusters.[14] The same nonlinearity is also reported on a Ru(0001) surface,[15] indicating a common growth mechanism shared by different metal surfaces. This is counterintuitive, since the carbon-metal interaction which determines graphene growth is different for different substrates. Furthermore, graphene growth on the same Ir(111) surface but for another orientation R30 has a different growth rate and nonlinear dependence.[15,16] The similar growth kinetics on different substrates and different growth kinetics on the same substrate found in experiment present a very attractive mystery.

While there are a variety of experimental works in this field, theoretical studies to reveal the growth kinetics are rare. Recently, by assuming that graphene islands grow homogeneously via the attachment of five-atom carbon (C_5) clusters,[17] a rate theory was developed to produce a quantitative account of the measured time-dependent carbon adatom density. Nevertheless, this model was mainly phenomenological and provided few atomic mechanisms. On the other hand, the large time-scale discrepancies between the attaching/detaching events at the atomic level and the growth behaviors at the macroscopic level, as well as those between the growth events involving different carbon clusters, make it hardly possible for brute-force simulations. To bridge the gap between the lattice mismatch pattern at the atomic level and macroscopic experimental growth kinetics, we have proposed a "standing-on-the-front" kinetic Monte Carlo (SOF-kMC) approach combined with density functional theory (DFT) calculations to perform multiscale simulations of the epitaxial growth of graphene in our earlier work.[18] There, we performed extensive DFT calculations to get the atomic details of different carbon clusters on the surface, and mainly focused on the growth behavior along R0 orientation on the Ir surface. The obtained growth rate shows nonlinear growth behavior in very good agreement with the experiments. By physical intuition, we proposed therein that lattice mismatch should play an important role in the nonlinear growth behavior. Although the mentioned work has made an important step toward the understanding of graphene growth kinetics, more interesting questions also arise. For instance, why is the growth exponent about 5 (experimental value is slightly larger than 5), but not 4 or 6? Is the picture that only C_5 successfully leads to graphene growth right? Why can similar nonlinear growth behavior be observed on different metal surfaces? Why is the nonlinear behavior so sensitive to the growth orientation? To answer these questions, a fundamental understanding of the epitaxial growth kinetics, relating the macroscopic growth behaviors to the atomic details, is necessary.

In the present paper, we apply the SOF-kMC approach combined with DFT calculations to address this problem. Generally, *lattice mismatch* between graphene and substrate will result in specific heterogeneity for graphene growth:[10,18] Taking the Ir(111) surface as a paradigm as shown in Fig. 1, DFT calculations showed that those *difficult sites* (DSs) nearly on top of the substrate atoms are hard to be attached by carbon atoms due to their high energy barriers of attachment, while other *easy sites* (ESs) are favorable for carbon atom attachment[18] as a result of much lower energy barriers. For different orientations (for example, R0 and R30 shown in Fig. 1), the locations of DSs and ESs can be derived by using simple geometric rules involving periodic and quasiperiodic structural motifs.[16] With such a simplification from the Morie pattern to a DS-ES model, we show that our multiscale approach can well reproduce the quintic growth kinetics observed experimentally for the R0 orientation. The underlying atomic mechanisms of this nontrivial growth kinetics, which can be revealed by detailed analysis of the involved growth events, are shown to be rather robust to the energy parameters associated with

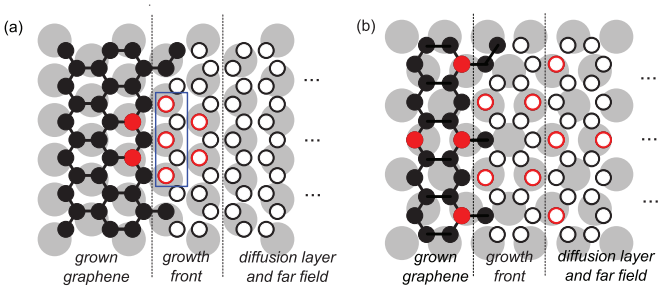

FIG. 1. (Color online) Schematic diagrams of lattice mismatch pattern on (a) R0 and (b) R30 orientations of Ir(001). Gray, black, and red circles represent the substrate atoms, ES, and DS, respectively. Solid (open) symbols stand for occupied (unoccupied) sites.

DSs. Such a robustness may explain why similar nonlinear growth kinetics can be founded on different metal substrates. Furthermore, studies on R30 orientation reveal that the growth mechanism is much sensitive to the distribution of DSs which is solely determined by the geometry of mismatched lattice. These findings bring us to a geometry-determined epitaxial growth mechanism of graphene on metal surfaces with lattice mismatch.

II. METHOD

The starting point of our SOF-kMC model is realizing that the growth kinetics are determined by the attachment and detachment processes of different carbon clusters at a well-defined growth front. The growth rate can be readily calculated if the incoming fluxes of all carbon clusters to the front and the involved rates of the attachment/detachment processes are available. In this regard, the whole surface lattice can be divided into four regions: The grown graphene sheet, growth front, diffusion layer, and far field, as illustrated briefly in Fig. 1 and in more detail in Fig. (S1) of the Supplemental Material.[20] In the far field, C_i clusters are assumed to be in equilibrium with each other, which allows us to estimate their populations on the surface according to $iC_1 \rightleftharpoons C_i$ with energies of each carbon species available. These clusters diffuse across the diffusion layer to the growth front, where they attach to the grown graphene with rate k_i^a, or detach from it with rate k_i^d. All of the energy parameters including $\epsilon_{i,D(E)}^{a(d)}$ associated with the attaching (detaching) events of C_i clusters on DSs (ESs) are all obtained from DFT calculations. Taking into account the clusters up to $i = 6$ and the lattice-mismatch-induced heterogeneity, one may then build up a kinetic model with 24 key events taking place on the growth front, namely, the attachment and detachment of $C_{i=1,\ldots,6}$ associated with DSs and ESs. Conventionally, a standard "event-list" kMC algorithm is ready for the simulation, which runs the dynamics by randomly determining what the next event is and when it will happen.[19] However, DFT calculations showed that there are very large (up to more than 10 orders of magnitude) discrepancies among the rates of these events, which render the direct kMC simulations very expensive. To overcome this difficulty, we have used a nested kMC algorithm, which finally makes the simulation of graphene growth a tractable problem and facilitates the calculation of the growth rate R_G.

TABLE I. Relative probabilities of growth events on R0 orientation for $n_1 = 0.01$ ML. 'A' and 'D' in brackets stand for attachment and detachment events, respectively. The $\sim$ symbol indicates a negligibly small value.

	ES(A)	ES(D)	DS(A)	DS(D)
C_1	0.342	0.219	$\sim$	1.79×10^{-3}
C_2	1.10×10^{-5}	3.27×10^{-3}	$\sim$	0.288
C_3	$\sim$	$\sim$	$\sim$	5.38×10^{-4}
C_4	$\sim$	$\sim$	0.139	$\sim$
C_5	$\sim$	$\sim$	7.51×10^{-3}	$\sim$
C_6	$\sim$	$\sim$	1.65×10^{-5}	$\sim$

More details of the SOF-kMC approach are described in the Supplemental Material.[20]

III. RESULTS AND DISCUSSIONS

To validate the SOF-kMC approach, we have simulated the dependence of R_G on n_1, the population of C_1, for graphene growth on the R0 orientation on the Ir surface.[18] The obtained curve can be very well fitted by a nonlinear growing function, $R_G \sim an_1^\gamma + b$, with the exponent $\gamma \simeq 5.25 \pm 0.02$ and a,b two constants. One notes that the value 5.25 agrees very well with the experiment,[15] which confirms the validity of our method. It is worthy to emphasize here that the growth exponent γ is not exactly 5, but slightly larger. This suggests that the picture proposed in the literature[14,17] that only C_5 clusters can effectively contribute to the front growth was not exactly right. Using our approach, it is feasible to perform a detailed analysis about the key events that contribute to the front growth. To this end, we have counted the numbers of each event that really happened in simulation of the front movement, as shown in Table I. Clearly, growth over ES is dominated by C_1 attachment. On the contrary, only large clusters (C_4, C_5, and C_6) can significantly attach to DS. The nonlinear growth behavior suggests that it is such DS-attaching events involving these relatively large clusters that control the growth process.

However, the results shown in Table I indicate that C_4 clusters attach more frequently to a DS than C_5 and C_6, which would suggest a nonlinear growth exponent $4 < \gamma < 5$. The simulation value $\gamma = 5.25$ seems to imply that C_4 actually contributes little to the front growth. To elucidate this point, we have traced the carbon atoms attached onto DSs. We find that although C_4 clusters can attach to DSs easily, almost all of them will detach via C_2 clusters such that the net contribution to the front growth is negligibly small. The attached C_5 clusters may also detach via small clusters, but an apparently nonvanishing amount of C_5 clusters will stay and thus provide a net contribution to the front growth. There is also a net contribution from C_6 clusters, but it is much less significant compared to C_5. In Table II, the detaching probabilities of attached C_4, C_5, and C_6 via small clusters, as well as their net attachment probabilities, are listed. Clearly, only C_5 and C_6 can stay on a DS stably and contribute to the front growth, and C_5 is significantly more important than C_6. Thus, the highly nonlinear growth behavior is a cooperative effect associated with the attachments of several large carbon clusters, rather than with a single species C_5.

TABLE II. Relative probabilities of DS events during the growth process on R0 orientation for $n_1 = 0.01$ ML. The $\sim$ symbol indicates a negligibly small value.

Species		C_4	C_5	C_6
Attachment		0.316	0.0171	6.58×10^{-5}
Detachment via	C_1	$\sim$	4.52×10^{-3}	$\sim$
	C_2	0.632	0.0287	1.39×10^{-4}
	C_3	$\sim$	1.11×10^{-3}	$\sim$
Net contribution		$\sim$	4.01×10^{-3}	1.94×10^{-5}

One should note that the growth process is rate limited by the DSs, i.e., only when all the DSs are filled stably can the front move forward. The above analysis reveals that only C_5 and C_6 clusters can effectively lead to front growth, i.e., stably fill the DSs, despite their low populations on the surface. To unravel this mystery, it is instructive to turn to the mismatch pattern shown in Fig. 1(a). For the zigzag-shape front enclosed by the rectangle, the three nearest DSs occupy two adjacent hexagons. Small clusters can hardly fill these three DSs simultaneously, thus they cannot be stably attached and will detach quickly before the next coming species. A C_4 cluster will fill two adjacent DSs and complete one hexagon, which makes the attaching events of C_4 on the DS possible as shown in Table I. However, the third unfilled DS may destabilize the front and these attached C_4 clusters will detach via smaller clusters with very small energy barriers as illustrated in Table II. On the contrary, a C_5 or C_6 cluster can cover these three DSs via a single attaching event, such that the resulting conformation is rather stable because the two adjacent hexagons are both completed and hence the front will grow successfully. The contribution of C_6 is much smaller simply because its population is much smaller on the surface. Therefore, it is the distribution of DSs over the surface that determines the dominant DS-attaching species, indicating a solely geometry effect. In a word, the observed nonlinear growth behavior of graphene actually bears a geometry-determined atomic mechanism.

If such a geometry-determined mechanism is right, one can expect that the nonlinear growth behavior should be robust to the heterogeneity level, which can be measured by the discrepancies between the energy parameters associated with a DS and those with an ES: $\Delta\epsilon_i^{a(d)} = \epsilon_{i,D}^{a(d)} - \epsilon_{i,E}^{a(d)}$. Although these values are fixed for the growth on an Ir surface, which can be noted as $\Delta\epsilon_{i0}^{a(d)}$, it is convenient for us to treat them as variable parameters in our simulation framework. This should be of particular importance, on the one hand, to get more new insights into the underlying mechanism of the lattice-mismatch-induced nonlinear growth, and on the other hand, to give predictions about the growth behaviors on other metal surfaces with similar lattice mismatch patterns but with different heterogeneity levels. The dependence of the growth exponent γ on $\alpha = \Delta\epsilon_i^{a(d)}/\Delta\epsilon_{i0}^{a(d)}$ is shown in Fig. 2. For $\alpha = 0$, the surface is essentially homogeneous and surely the growth process would be determined by C_1 which corresponds to $\gamma = 1$. With increasing α, lattice mismatch takes effect and carbon clusters are required to fill the DSs, which leads to nonlinear growth with $\gamma > 1$. Remarkably, two distinct

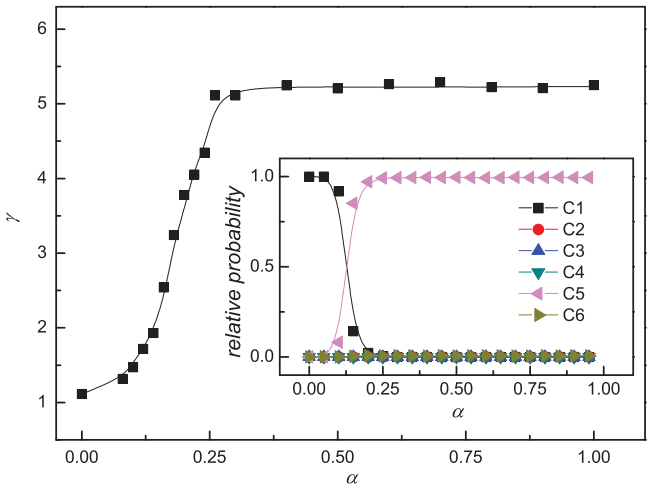

FIG. 2. (Color online) The dependence of growth exponent γ on heterogeneity level α for R0 orientation. Inset: Net contribution of different carbon species (in relative probability).

regimes are observed with increasing α: For α less than a certain threshold value α_c, the exponent γ is rather sensitive to the change of α; while for $\alpha > \alpha_c$, γ saturates to a nearly constant value same as that for $\alpha = 1$. This validates that if lattice-mismatch-induced heterogeneity is strong enough, the growth behavior is indeed robust to it and solely determined by the geometry.

We have also analyzed the net contributions (probabilities) of different C_i species to the front growth as functions of α. As shown in the inset of Fig. 2, a narrow transition window exists around α_c. For small α, the front growth is dominated by C_1, the net probability of which decreases sharply within the window. On the contrary, the contribution of C_5 increases sharply in the window and becomes dominate for $\alpha > \alpha_c$. Similar to the case of $\alpha = 1$, as demonstrated in Table I, the contributions of C_i with $(i = 2,3,4)$ to the front growth is negligible. The fact that only C_5 and C_6 (much smaller) can contribute to the front growth for relatively large α further demonstrates the validity of a geometry-determined mechanism. We note here that the robustness of γ to the change of $\epsilon_{i,D}^{a(d)}$ for each single growth event has also been tested.[20]

The above geometry-dependent picture raises an interesting question: How would the growth kinetics change if the graphene grew on another orientation, e.g., R30? As shown in Fig. 1(b), the mismatch pattern along R30 is quite different from that along R0, say, the DSs are separated farther from each other. To address this issue, we have performed similar simulations by using specific energy parameters $\epsilon_{i,D(E)}^{a(d)}$ for the R30 direction obtained by DFT calculations. The dependence of R_G on n_1 is shown in Fig. 3(a), which can be well fitted by $R_G = an_1^{\gamma} + b$ with an exponent $\gamma = 2.01 \pm 0.02$. The inset presents the relative probability of different growth events. Clearly, DSs can now be filled successfully by C_2 clusters, which dominate the growth on R30. Contrary to the R0 case, contributions of the carbon clusters with $i \geqslant 3$ are not observable. We have also investigated how the growth kinetics depends on the heterogeneity level. The results similar to Fig. 2 are shown in Fig. 3(b), where the exponent γ is drawn as a

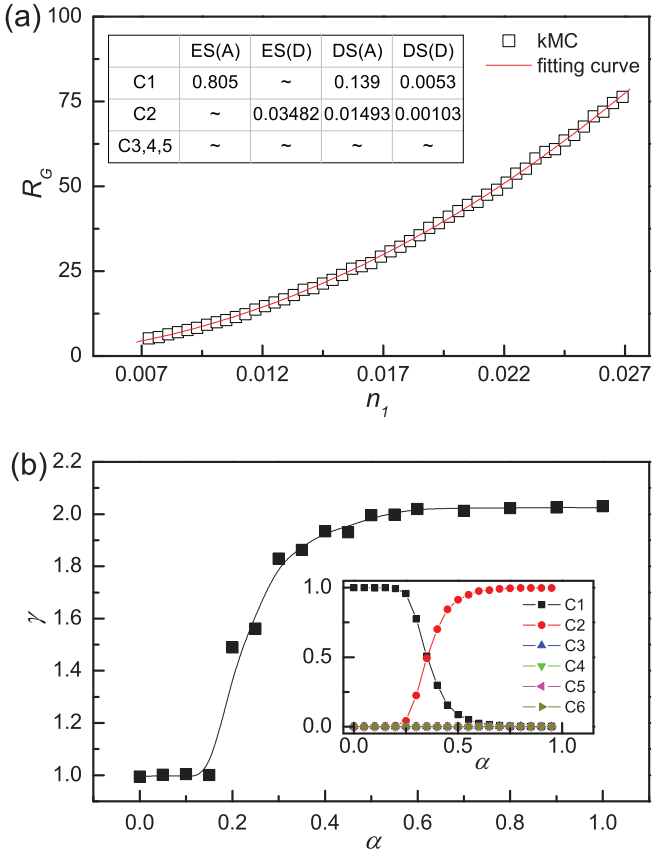

FIG. 3. (Color online) (a) Dependence of R_G on n_1 (in ML) on R30 orientation. Inset: Relative probabilities of growth events. (b) Growth exponent γ as a function of heterogeneity level α for R30 orientation. Inset: Net contribution of different carbon species (in relative probability).

function of α. There is also an increasing of γ with α, but now γ saturates to a much smaller value 2.0 compared to $\gamma = 5.25$ in the R0 case. As shown in the inset, only C_1 and C_2 matter for this orientation, while the former dominates for small α and the latter dominates for large α.

The observed exponent $\gamma \simeq 2$ for R30 as well as its robustness against the parameter α can also be elucidated by the same geometry-determined mechanism as that for R0. As shown in Fig. 1(b), DS on the front are separated from each other with at least three ESs in between. Clearly, DSs in the growth front can be filled by C_2 clusters successfully. When one DS is filled, the hexagon it belongs to is completed and stable which is not influenced by the other DSs nearby. The front thus moves forward when the DSs are all filled by C_2 species. The key difference between R0 and R30 directions is the correlation between adjacent DSs, which is strong in the former and weak in the latter. Note that this correlation is simply determined by the mismatch geometry.

IV. CONCLUSION

In summary, a geometry-determined epitaxial growth mechanism of graphene on a metal surface with lattice mismatch has been revealed in a general statistical mechanics framework by using a multiscale SOF-kMC approach. When sites difficult for monomer adsorption exist, growth kinetics can be well predicted simply by checking the mismatch pattern. We believe that our finding can inspire more experimental work and open new perspectives for theoretical studies on epitaxial growth kinetics.

ACKNOWLEDGMENTS

We are grateful to Prof. Zhenyu Zhang for helpful discussions. This work is supported by MOST (2011CB921404), NSFC (21125313, 20933006, 91027012, 21173202, 21121003, and 21222304), CUSF (WK2340000011), CAS(KJCX2-YWW22, XDB01020300), and USTC-SCC, SCCAS, and Shanghai Supercomputer Centers.

*hzhlj@ustc.edu.cn
†zyli@ustc.edu.cn

[1] K. S. Novoselov, A. K. Geim, S. V. Morozov, D. Jiang, Y. Zhang, S. V. Dubonos, I. V. Grigorieva, and A. A. Firsov, Science **306**, 666 (2004).
[2] D. R. Dreyer, S. Park, C. W. Bielawski, and R. S. Ruoff, Chem. Soc. Rev. **39**, 228 (2010).
[3] P. W. Sutter, J.-I. Flege, and E. A. Sutter, Nat. Mater. **7**, 406 (2008).
[4] J. Coraux, A. T. N'Diaye, C. Busse, and T. Michely, Nano Lett. **8**, 565 (2008).
[5] K. S. Kim, Y. Zhao, H. Jang, S. Y. Lee, J. M. Kim, K. S. Kim, J.-H. Ahn, P. Kim, J.-Y. Choi, and B. H. Hong, Nature **457**, 706 (2009).
[6] Z. Li, P. Wu, C. Wang, X. Fan, W. Zhang, X. Zhai, C. Zeng, Z. Li, J. Yang, and J. Hou, ACS Nano **5**, 3385 (2011).
[7] X. Li, W. Cai, J. An, S. Kim, J. Nah, D. Yang, R. Piner, A. Velamakanni, I. Jung, E. Tutuc *et al.*, Science **324**, 1312 (2009).
[8] Y. S. Dedkov, M. Fonin, U. Rüdiger, and C. Laubschat, Phys. Rev. Lett. **100**, 107602 (2008).
[9] A. Reina, X. Jia, J. Ho, D. Nezich, H. Son, V. Bulovic, M. S. Dresselhaus, and J. Kong, Nano Lett. **9**, 30 (2008).
[10] S. Marchini, S. Günther, and J. Wintterlin, Phys. Rev. B **76**, 075429 (2007).
[11] I. Pletikosić, M. Kralj, P. Pervan, R. Brako, J. Coraux, A. T. N'Diaye, C. Busse, and T. Michely, Phys. Rev. Lett. **102**, 056808 (2009).
[12] P. Lacovig, M. Pozzo, D. Alfè, P. Vilmercati, A. Baraldi, and S. Lizzit, Phys. Rev. Lett. **103**, 166101 (2009).
[13] Z. Li, W. Zhang, X. Fan, P. Wu, C. Zeng, Z. Li, X. Zhai, J. Yang, and J. Hou, J. Phys. Chem. C **116**, 10557 (2012).
[14] E. Loginova, N. C. Bartelt, P. J. Feibelman, and K. F. McCarty, New J. Phys. **10**, 093026 (2008).
[15] E. Loginova, N. C. Bartelt, P. J. Feibelman, and K. F. McCarty, New J. Phys. **11**, 063046 (2009).
[16] E. Loginova, S. Nie, K. Thürmer, N. C. Bartelt, and K. F. McCarty, Phys. Rev. B **80**, 085430 (2009).
[17] A. Zangwill and D. D. Vvedensky, Nano Lett. **11**, 2092 (2011).
[18] P. Wu, H. Jiang, W. Zhang, Z. Li, Z. Hou, and J. Yang, J. Am. Chem. Soc. **134**, 6045 (2012).
[19] D. T. Gillespie, J. Phys. Chem. **81**, 2340 (1977).
[20] See Supplemental Material at http://link.aps.org/supplemental/10.1103/PhysRevB.88.054304 for details of the SOF-kMC approach, and for the robustness of growth kinetics to the energy parameter of single growth events.